

New limits on $\tan\beta$ for 2HDMs with Z_2 symmetry

Dipankar Das*

Saha Institute of Nuclear Physics, 1/AF Bidhan Nagar, Kolkata 700064, India

ABSTRACT: In two-Higgs-doublet models with exact Z_2 symmetry, putting $m_h \simeq 125$ GeV at the alignment limit, the following limits on the heavy scalar masses are obtained from the conditions of unitarity and stability of the scalar potential: $m_H, m_A, m_{H^\pm} < 1$ TeV and $1/8 < \tan\beta < 8$. The constraints from $b \rightarrow s\gamma$ and neutral meson mass differences, when superimposed on the unitarity constraints, put a tighter lower limit on $\tan\beta$ depending on m_{H^\pm} . It has also been shown that larger values of $\tan\beta$ can be allowed by introducing soft breaking term in the potential at the expense of a correlation between m_H and the soft breaking parameter.

1 Introduction

Extension of the Standard Model (SM) scalar sector is a common practice in constructing new physics models to address the shortcomings of the SM. Two-Higgs-doublet models (2HDMs) [1] are amongst the simplest of extensions that add only one extra $SU(2)$ doublet to the SM scalar sector. The tree level value of the electroweak ρ -parameter remains unity for these types of extensions. In a general 2HDM, however, both the doublets (Φ_1 and Φ_2) can couple to each type of fermions. Consequently there will be two Yukawa matrices which, in general, are not diagonalizable simultaneously. This will introduce new flavor changing neutral currents (FCNC) mediated by neutral Higgses. It was shown by Glashow and Weinberg [2] and independently by Paschos [3] that Higgs mediated FCNC can be avoided altogether if fermions of a particular charge get their masses from the vacuum expectation value (vev) of a single scalar doublet. This prescription was realized by employing a Z_2 symmetry under which one of the doublet is odd. Then there are four different possibilities for assigning Z_2 parities to the fermions so that Glashow-Weinberg-Paschos theorem is satisfied. Following the usual convention, we shall always call Φ_2 the doublet which couples to the up-type quarks. This leads to the following four types of 2HDMs:

- Type I: all quarks and leptons couple to only one scalar doublet Φ_2 ;
- Type II: Φ_2 couples to up-type quarks, while Φ_1 couples to down-type quarks and charged leptons (minimal supersymmetry conforms to this category);
- Type X or lepton specific: Φ_2 couples to all quarks, while Φ_1 couples to all leptons;
- Type Y or flipped: Φ_2 couples to up-type quarks and leptons, while Φ_1 couples to down-type quarks.

Now that a light Higgs boson has been observed by the ATLAS and CMS Collaborations of the CERN Large Hadron Collider (LHC), the time is appropriate to revisit the constraints on 2HDM parameter space arising from the requirement of perturbative unitarity associated with the scattering amplitudes together with the complementary constraints coming from the flavor observables. Requirement of unitarity is a consequence of

*d.das@saha.ac.in

probability conservation at the quantum level. Essentially, one takes tree level amplitudes of appropriate sets of scattering processes, and impose the unitarity condition that the s -wave scattering amplitude $|a_0| < 1$. Equivalence theorem allows us to make the calculations easier by replacing the longitudinal gauge with the corresponding Goldstone bosons. In the context of the SM, Lee, Quigg and Thacker (LQT) had put an upper bound on the Higgs boson mass, $m_h < m_{\text{LQT}} = (8\pi\sqrt{2}/3G_F)^{1/2} \sim 1 \text{ TeV}$ [4]. The LQT-type analyses were later carried out to constrain the nonstandard parameter spaces for several extensions of the SM scalar sector. Detailed analyses of these constraints in the 2HDM context already exist in the literature [5–11]. In this paper, we study the consequences of adding two additional inputs to the existing analyses: (i) we use $m_h \simeq 125 \text{ GeV}$ as input, which was an unknown parameter earlier, and also note that the fitted values of the couplings of the Higgs boson from the observed signal strengths into various fermion and gauge boson channels show close conformity to the *alignment limit*, and (ii) the restrictions coming from two crucial flavor observables, namely, branching ratio of $b \rightarrow s\gamma$ and the meson mass splittings have been superimposed on the unitarity constraints. We observe that for a large class of 2HDM with *exact* Z_2 symmetry, the unitarity and flavor constraints *together* allow a rather restricted zone for m_{H^\pm} and $\tan\beta$, thus imposing *new* constraints on these parameters. The limits on $\tan\beta$ are now independent of any other parameter, its upper limit coming from unitarity and the lower limit from flavor observables. We study these constraints in all four types of 2HDMs mentioned earlier. The limits are the strongest when the Z_2 symmetry is exact, while they get diluted by the soft symmetry breaking terms. We also comment on what happens when instead of Z_2 , softly broken $U(1)$ symmetry is considered.

This paper is organized as follows: in Section 2 we discuss the 2HDM scalar potential and the relevance of the alignment limit. Section 3 is divided into two parts. In the first part, we discuss the constraints arising from the requirements of unitarity and stability. Conclusions obtained from this part are independent of the Yukawa structure of the model. In the second part, we revisit the Yukawa sector dependent constraints originating from flavor data and superimpose the result on the unitarity constraints. Finally, the important findings are summarized in Section 4.

2 The scalar potential

The general scalar potential of a 2HDM invariant under a Z_2 ($\Phi_2 \rightarrow -\Phi_2$) symmetry can be written as [12]

$$\begin{aligned}
V = & \lambda_1 \left(\Phi_1^\dagger \Phi_1 - \frac{v_1^2}{2} \right)^2 + \lambda_2 \left(\Phi_2^\dagger \Phi_2 - \frac{v_2^2}{2} \right)^2 + \lambda_3 \left(\Phi_1^\dagger \Phi_1 + \Phi_2^\dagger \Phi_2 - \frac{v_1^2 + v_2^2}{2} \right)^2 \\
& + \lambda_4 \left((\Phi_1^\dagger \Phi_1)(\Phi_2^\dagger \Phi_2) - (\Phi_1^\dagger \Phi_2)(\Phi_2^\dagger \Phi_1) \right) + \lambda_5 \left(\text{Re } \Phi_1^\dagger \Phi_2 - \frac{v_1 v_2}{2} \right)^2 + \lambda_6 \left(\text{Im } \Phi_1^\dagger \Phi_2 \right)^2, \quad (1)
\end{aligned}$$

where, the bilinear term proportional to λ_5 breaks the Z_2 symmetry softly. This soft breaking term, in its conventional parametrization, is written as $-m_{12}^2(\Phi_1^\dagger \Phi_2 + \Phi_2^\dagger \Phi_1)$. The connection between m_{12}^2 and λ_5 is given by [13]

$$m_{12}^2 = \frac{\lambda_5}{2} v_1 v_2. \quad (2)$$

Defining $\tan\beta \equiv v_2/v_1$ to be the ratio of the two vevs, we also remember that it is the combination $m_{12}^2/(\sin\beta \cos\beta)$, not m_{12}^2 itself, which controls the nonstandard masses [14]. In view of these facts, λ_5 , rather than m_{12}^2 , constitutes a convenient parameter that can track down the effect of soft breaking. Note that, unlike the *inert* case, Eq. (1) implicitly assumes that the Z_2 symmetry is also broken spontaneously, *i.e.*, both the doublets receive vevs. In this article, we shall only consider 2HDMs where the value of $\tan\beta$ is nonzero and finite. We have also assumed that all the potential parameters are real, *i.e.*, CP symmetry is exact in the scalar potential. The last assumption allows us to define electrically neutral mass eigenstates which are also eigenstates of CP. Here there will be a total of five physical scalars: a pair of CP-even scalars (h and H with $m_H > m_h$), one CP-odd scalar (A) and a pair of charged scalars (H^\pm). For the transition into the mass basis, one needs to rotate the original fields in Eq. (1) by an angle β in the charged and the CP-odd sectors, whereas, the rotation

angle involved in the CP-even sector is denoted by α . The latter angle is defined through the relation

$$\tan 2\alpha = \frac{2(\lambda_3 + \frac{\lambda_5}{4})v_1v_2}{\lambda_1v_1^2 - \lambda_2v_2^2 + (\lambda_3 + \frac{\lambda_5}{4})(v_1^2 - v_2^2)}. \quad (3)$$

Note that there were eight parameters to start with: v_1 , v_2 and 6 lambdas. One can trade v_1 and v_2 for $v = \sqrt{v_1^2 + v_2^2}$ and $\tan \beta$. All the lambdas except λ_5 may be traded for 4 physical Higgs masses and α . The relations between these two equivalent sets of parameters are given below :

$$\lambda_1 = \frac{1}{2v^2 \cos^2 \beta} \left[m_H^2 \cos^2 \alpha + m_h^2 \sin^2 \alpha - \frac{\sin \alpha \cos \alpha}{\tan \beta} (m_H^2 - m_h^2) \right] - \frac{\lambda_5}{4} (\tan^2 \beta - 1), \quad (4a)$$

$$\lambda_2 = \frac{1}{2v^2 \sin^2 \beta} \left[m_h^2 \cos^2 \alpha + m_H^2 \sin^2 \alpha - \sin \alpha \cos \alpha \tan \beta (m_H^2 - m_h^2) \right] - \frac{\lambda_5}{4} (\cot^2 \beta - 1), \quad (4b)$$

$$\lambda_3 = \frac{1}{2v^2} \frac{\sin \alpha \cos \alpha}{\sin \beta \cos \beta} (m_H^2 - m_h^2) - \frac{\lambda_5}{4}, \quad (4c)$$

$$\lambda_4 = \frac{2}{v^2} m_{H^\pm}^2, \quad (4d)$$

$$\lambda_6 = \frac{2}{v^2} m_A^2. \quad (4e)$$

Among these, $v = 246$ GeV is already known and if it is assumed that the lightest CP-even Higgs is what has been observed at the LHC, then $m_h = 125$ GeV is also known. The rest of the parameters need to be constrained from theoretical as well as experimental considerations.

The first simplification occurs if one keeps in mind that the experimental values of the Higgs signal strengths into different decay channels are increasingly leaning towards the corresponding SM predictions [15, 16]. In the 2HDM context, this implies the *alignment* condition [14]

$$\sin(\beta - \alpha) \approx 1, \quad (5)$$

which means, h will have the exact same tree-level couplings with the vector bosons and fermions as in the SM. In view of the recent global fits for 2HDMs using the LHC Higgs data, Eq. (5) is a reasonable assumption [17–22].

Next, one has to ensure that there should not exist any direction in the field space along which the potential of Eq. (1) becomes infinitely negative, *i.e.*, the potential is bounded from below. The necessary and sufficient conditions for this can be found to be [23, 24]

$$\lambda_1 + \lambda_3 > 0, \quad (6a)$$

$$\lambda_2 + \lambda_3 > 0, \quad (6b)$$

$$2\lambda_3 + \lambda_4 + 2\sqrt{(\lambda_1 + \lambda_3)(\lambda_2 + \lambda_3)} > 0, \quad (6c)$$

$$2\lambda_3 + \frac{\lambda_5 + \lambda_6}{2} - \frac{|\lambda_5 - \lambda_6|}{2} + 2\sqrt{(\lambda_1 + \lambda_3)(\lambda_2 + \lambda_3)} > 0. \quad (6d)$$

To obtain the constraints from tree-unitarity, we construct an S -matrix using different two-body states to label its different rows and columns. The $\ell = 0$ partial wave amplitudes for different $2 \rightarrow 2$ scattering processes constitute the elements of this S -matrix. The explicit expressions for the eigenvalues of this matrix are listed below [5–8]:

$$a_1^\pm = 3(\lambda_1 + \lambda_2 + 2\lambda_3) \pm \sqrt{9(\lambda_1 - \lambda_2)^2 + \left(4\lambda_3 + \lambda_4 + \frac{\lambda_5 + \lambda_6}{2}\right)^2}, \quad (7a)$$

$$a_2^\pm = (\lambda_1 + \lambda_2 + 2\lambda_3) \pm \sqrt{(\lambda_1 - \lambda_2)^2 + \frac{1}{4}(2\lambda_4 - \lambda_5 - \lambda_6)^2}, \quad (7b)$$

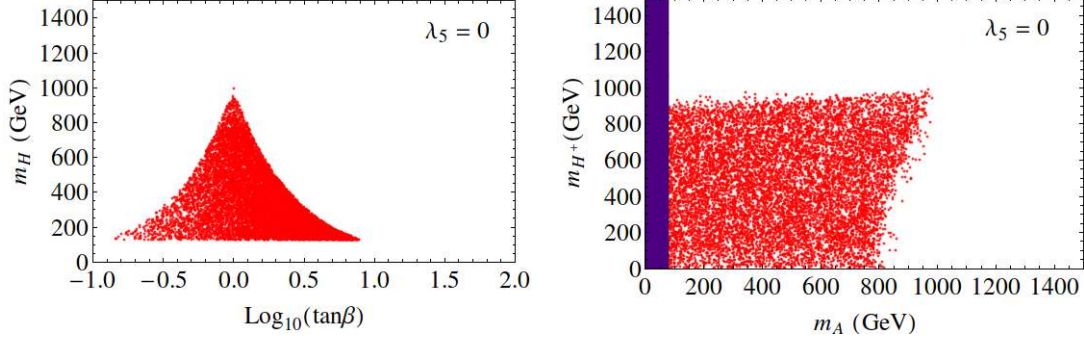


Figure 1: Allowed region from unitarity and stability for exact Z_2 symmetry. In the right panel, the dark (purple) shaded region is excluded from direct search [25].

$$a_3^\pm = (\lambda_1 + \lambda_2 + 2\lambda_3) \pm \sqrt{(\lambda_1 - \lambda_2)^2 + \frac{1}{4}(\lambda_5 - \lambda_6)^2}, \quad (7c)$$

$$b_1 = 2\lambda_3 - \lambda_4 - \frac{1}{2}\lambda_5 + \frac{5}{2}\lambda_6, \quad (7d)$$

$$b_2 = 2\lambda_3 + \lambda_4 - \frac{1}{2}\lambda_5 + \frac{1}{2}\lambda_6, \quad (7e)$$

$$b_3 = 2\lambda_3 - \lambda_4 + \frac{5}{2}\lambda_5 - \frac{1}{2}\lambda_6, \quad (7f)$$

$$b_4 = 2\lambda_3 + \lambda_4 + \frac{1}{2}\lambda_5 - \frac{1}{2}\lambda_6, \quad (7g)$$

$$b_5 = 2\lambda_3 + \frac{1}{2}\lambda_5 + \frac{1}{2}\lambda_6, \quad (7h)$$

$$b_6 = 2(\lambda_3 + \lambda_4) - \frac{1}{2}\lambda_5 - \frac{1}{2}\lambda_6. \quad (7i)$$

The requirement of tree-unitarity then restricts each of the above eigenvalues as

$$|a_i^\pm|, |b_i| \leq 16\pi. \quad (8)$$

Now it is the time to investigate how the constraints from unitarity and stability restrict the parameter space in the *alignment limit* defined by Eq. (5).

3 Constraints on the 2HDM parameter space

To begin with, we consider the case when the Z_2 symmetry is exact in the scalar potential *i.e.*, $\lambda_5 = 0$. For this, we have generated millions of random points in the $\{\tan \beta, m_H, m_A, m_{H^+}\}$ space. The individual parameters have been varied in the following range:

$$\tan \beta \in [0.1, 100], \quad m_H \in [125, 2000], \quad m_A \in [0, 2000], \quad m_{H^+} \in [0, 2000]. \quad (9)$$

Those points which successfully negotiate the unitarity and stability bounds have been plotted in Fig. 1. Some noteworthy features are listed below :

- From the left panel, one can read the limit on $\tan \beta$, $1/8 < \tan \beta < 8$.
- Strong correlation exists between the upper limit of m_H and $\tan \beta$.
- Limits on the masses are, $m_H, m_A, m_{H^+} < 1$ TeV.

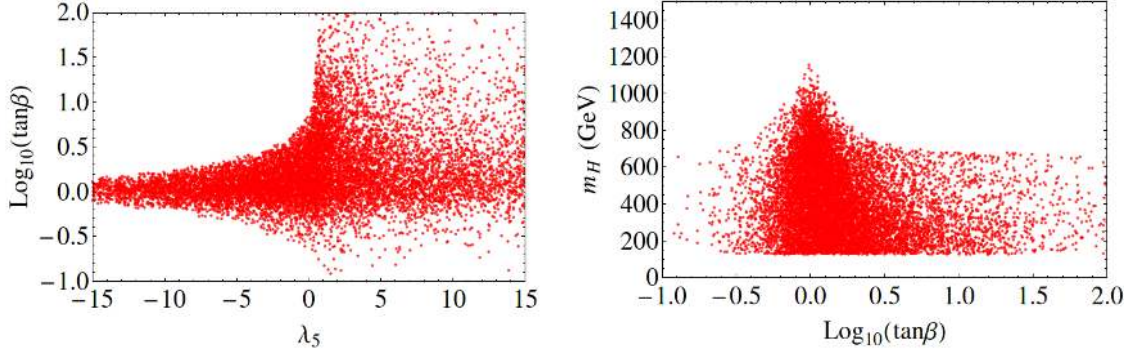


Figure 2: *Relaxation of the unitarity and stability constraints on $\tan\beta$ in the presence of soft breaking. In the right panel, the vertical width of the tail in the region where $\tan\beta$ is much away from unity is caused by the variation of λ_5 in the range $[-15, 15]$.*

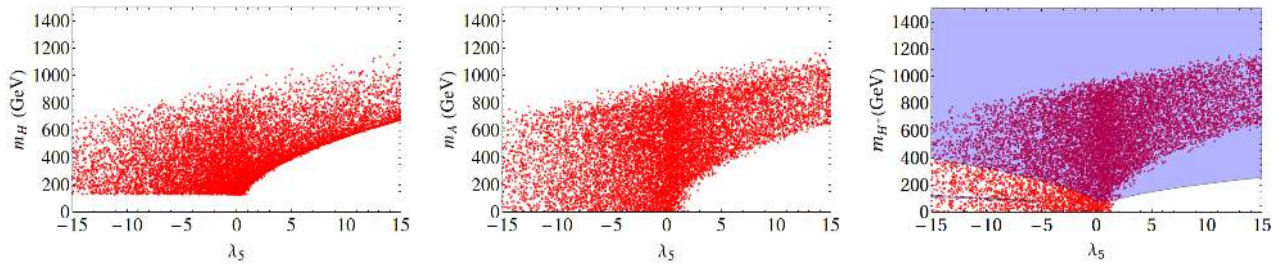


Figure 3: *Effect of soft breaking on the constraints on the nonstandard masses. The (light blue) shaded region in the rightmost panel represents the combined allowed region from direct search and the diphoton signal strength at 95% C.L.*

The reason for the above features can be traced back to the eigenvalues of Eq. (7). First two constraints for boundedness in Eq. (6) can be combined into

$$\lambda_1 + \lambda_2 + 2\lambda_3 > 0. \quad (10)$$

This, then together with the condition $|a_1^\pm| < 16\pi$, implies

$$0 < \lambda_1 + \lambda_2 + 2\lambda_3 < \frac{16\pi}{3}, \quad (11)$$

$$\Rightarrow 0 < \left(m_H^2 - \frac{1}{2}\lambda_5 v^2\right) (\tan^2\beta + \cot^2\beta) + 2m_h^2 < \frac{32\pi v^2}{3}, \quad (12)$$

where the last expression is obtained from the previous one by using Eq. (4) in the alignment limit. Keeping in mind that $m_H > 125$ GeV, this will put a limit on $\tan\beta$ (as well as $\cot\beta$) when $\lambda_5 = 0$. Since the minimum value of $(\tan^2\beta + \cot^2\beta)$ is 2 when $\tan\beta = 1$, the maximum possible value of m_H occurs at $\tan\beta = 1$. In summary, the inequality (12) explains the $\tan\beta$ dependent bound on m_H as depicted in the left panel of Fig. 1.

Eq. (12) also implies that the restriction on $\tan\beta$ will be lifted for $1/2\lambda_5 v^2 > (m_H^2)_{\min} = (125 \text{ GeV})^2$. Once this condition is satisfied, m_H^2 will have the chance to saturate to $1/2\lambda_5 v^2$ making the difference between them to vanish in Eq. (12). In fact, to a very good approximation, one can use

$$m_H^2 \approx 1/2\lambda_5 v^2 \quad (13)$$

for $\tan\beta > 5$.

To understand the restrictions on m_A and m_{H^+} , we use the triangle inequality to note the following :

$$|b_1 - b_3| \equiv 3|\lambda_6 - \lambda_5| < 32\pi, \quad \Rightarrow |m_A^2 - \frac{1}{2}\lambda_5 v^2| < \frac{16\pi v^2}{3}, \quad (14a)$$

$$|b_6 - b_3| \equiv 3|\lambda_4 - \lambda_5| < 32\pi, \quad \Rightarrow |m_{H^+}^2 - \frac{1}{2}\lambda_5 v^2| < \frac{16\pi v^2}{3}. \quad (14b)$$

Because of Eqs. (14a) and (14b) one expects to put limits on m_A and m_{H^+} respectively, when $\lambda_5 = 0$. Additionally, note that due to the inequality

$$|b_1 - b_6| \equiv 3|\lambda_6 - \lambda_4| < 32\pi, \quad \Rightarrow |m_A^2 - m_{H^+}^2| < \frac{16\pi v^2}{3}, \quad (15)$$

it is expected that the splitting between m_A and m_{H^+} will be *always* restricted in a 2HDM. It is also interesting to note that the conclusions obtained from Eqs. (14a), (14b) and (15) *do not* depend on the imposition of the alignment condition.

Next we shall investigate the implications of the soft breaking parameter on these constraints. We have varied λ_5 in the range $[-15, 15]$ for this purpose. From Eq. (12) one can observe that the space for $\tan\beta$ is squeezed further if $\lambda_5 < 0$ but the bound is relaxed if $\lambda_5 > 0$. This feature emerges from the left panel of Fig. 2. One can also see from Eq. (12) that m_H^2 must follow $1/2\lambda_5 v^2$ if $\tan\beta$ moderately deviates from unity. This feature is reflected by the horizontal tail in the right panel of Fig. 2 on both sides of the peak. The vertical width of the tail is caused by the variation of λ_5 in the range $[-15, 15]$. On the other hand, from Eqs. (14a), (14b) and (12), it should be noted that the upper bounds on the nonstandard scalar masses will be relaxed for $\lambda_5 > 0$ but will get tighter for $\lambda_5 < 0$. Fig. 3 reflects these features where one can see that this dependence is rather weak. It is worth mentioning at this point that if one uses a softly broken $U(1)$ symmetry instead of the usual Z_2 symmetry, the soft breaking parameter gets related to the pseudoscalar mass as $m_A^2 = 1/2\lambda_5 v^2$. Consequently, the correlation between m_H and λ_5 in the leftmost panel of Fig. 3 transforms into the degeneracy between m_H and m_A . Detailed analysis of the scalar sector, for the softly broken $U(1)$ scenario, has been carried out in [26, 27].

It is also important to note that the production as well as the tree-level decay widths of h remain unaltered from the corresponding SM expectations due to the imposition of alignment limit of Eq. (5). But the loop induced decay modes of h , such as $h \rightarrow \gamma\gamma$ and $h \rightarrow Z\gamma$, will pick up additional contributions due the presence of the charged scalar in loops. For example, the diphoton signal strength ($\mu_{\gamma\gamma}$), in general, depends on both λ_5 and m_{H^+} [13]. The current measurement by CMS gives $\mu_{\gamma\gamma} = 1.14^{+0.26}_{-0.23}$ [28], whereas ATLAS measures $\mu_{\gamma\gamma}$ to be 1.17 ± 0.27 [29]. In addition to this, the direct search limit of $m_{H^+} > 80$ GeV [25] should also be taken into account. Considering all of these experimental constraints, the allowed region at 95% C.L. has been shaded (in light blue) in the rightmost panel of Fig. 3. Only those points that lie within the shaded region survive both the theoretical and experimental constraints.

3.1 Yukawa sector and flavor constraints

Now we shall concentrate on the constraints on the charged scalar mass (m_{H^+}), imposed by the measured values of $b \rightarrow s\gamma$ branching ratio [30] and neutral meson mass differences (ΔM) [31]. Since we are concerned with the quark sector only, the constraints will be the same for Type I and Type X models. The same is true for Type II and Type Y models. In the following, we spell out the relevant parts of the charged scalar Yukawa interaction:

$$\mathcal{L}_{H^+}^{(\text{I or X})} = \left[\frac{\sqrt{2}H^+}{v} \cot\beta \left\{ \bar{u}_R (D_u V) d_L - \bar{u}_L (V D_d) d_R \right\} + \text{h.c.} \right], \quad (16a)$$

$$\mathcal{L}_{H^+}^{(\text{II or Y})} = \left[\frac{\sqrt{2}H^+}{v} \left\{ \cot\beta \bar{u}_R (D_u V) d_L + \tan\beta \bar{u}_L (V D_d) d_R \right\} + \text{h.c.} \right], \quad (16b)$$

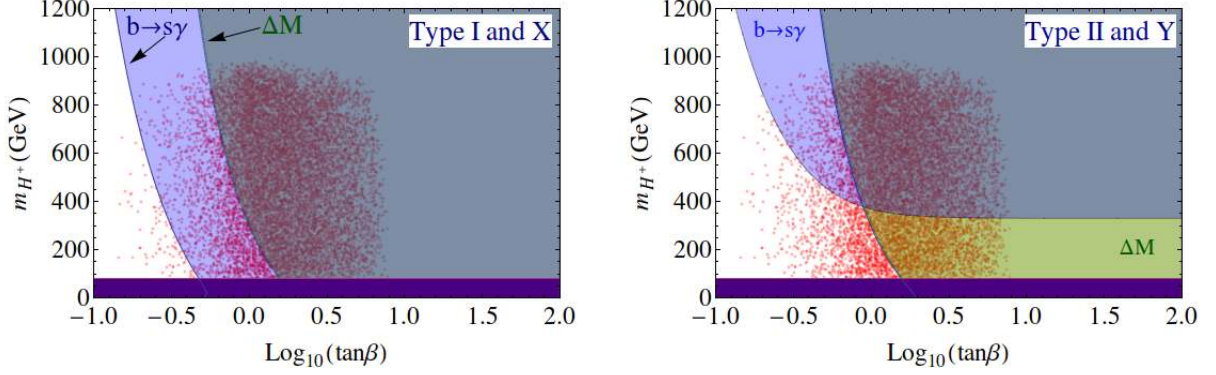


Figure 4: Constraints on $\tan\beta$ and the charged Higgs mass from unitarity and flavor physics. The left panel corresponds to Type I and X and the right panel to Type II and Y scenarios. The lower horizontal dark (purple) strip in both the panels corresponds to the direct search limit of 80 GeV [25]. The lighter shades represent allowed regions from individual flavor observables. The scattered points are allowed from unitarity and stability for 2HDMs with exact Z_2 symmetry.

where, V is the CKM matrix and $D_{u,d}$ are diagonal mass matrices in the up- and down-quark sectors respectively. In writing Eq. (16), we have suppressed the flavor indices. Thus u and d should be interpreted as three element column matrices.

For the process $b \rightarrow s\gamma$, the major new physics contributions come from charged scalar loops. We have added the new physics contribution to the SM one at the amplitude level and therefore have taken the interference into account. The branching ratio is then compared with the experimental value, $(3.55 \pm 0.26) \times 10^{-4}$ [30], to obtain the allowed region at 95% C.L. in Fig. 4. As can be seen from Eq. (16b), for Type II and Y models, in the charged Higgs Yukawa interaction, the up-type Yukawa coupling is multiplied by $\cot\beta$ while the down-type Yukawa is multiplied by $\tan\beta$. Their product is responsible for setting $\tan\beta$ -independent limit¹ $m_{H^+} > 320$ GeV for $\tan\beta > 1$ [33–35]. This feature has been depicted in the right panel of Fig. 4. In Type I and X models, on the other hand, each of these couplings picks up a $\cot\beta$ factor. This is why there is essentially no bound on m_{H^+} for $\tan\beta > 1$ in these models [34]. This character of Type I and X models emerges from the left panel of Fig. 4.

The dominant new physics contributions to neutral meson mass differences come from the charged scalar box diagrams. Note that, the constraint arising from ΔM in the m_{H^+} - $\tan\beta$ plane, is slightly stronger than that from the precision measurement of the $Z \rightarrow b\bar{b}$ branching ratio [35]. In Fig. 4, allowed regions have been shaded assuming that the new physics contributions saturate the experimental values of ΔM [31]. Since the amplitudes for the new box diagrams receive prevailing contributions from the up-type quark masses which, for all four variants of 2HDMs, comes with a $\cot\beta$ prefactor, the overall charged scalar contribution to the amplitude goes as $\cot^4\beta$ due to the presence of four charged scalar vertices in the box diagram. Not surprisingly, ΔM offers a stronger constraint than $b \rightarrow s\gamma$ for $\tan\beta < 1$ because, in this region, the new physics amplitude for the latter goes as $\cot^2\beta$.

Things become more interesting when the above flavor constraints are superimposed on top of the constraints from unitarity and stability. Most stringent constraints are obtained when Z_2 symmetry is exact in the scalar potential, *i.e.*, $\lambda_5 = 0$. In Fig. 4, the scattered points span the region allowed by the combined constraints of unitarity and stability for the case of exact Z_2 symmetry. Only those points which lie within the common shaded region survive when all the constraints are imposed. For 2HDMs of all four types, one can read the

¹Recently this bound has been changed to $m_{H^+} > 480$ GeV using the NNLO result along with the updated experimental value [32]. This means that the $b \rightarrow s\gamma$ boundary on the right panel of Fig. 4 will be shifted upwards slightly. But this will hardly modify the lower bound on $\tan\beta$ which mainly comes from ΔM .

bound on $\tan\beta$ as

$$0.5 < \tan\beta < 8. \tag{17}$$

However, in order to allow a lighter charged scalar in the ballpark of 400 GeV or below, one must require $1 < \tan\beta < 8$. It should be remembered that, the lower bound on $\tan\beta$ mainly comes from the flavor data, whereas the upper limit, for the case of exact Z_2 symmetry, is dictated by unitarity and stability. In the presence of a soft breaking parameter, the upper bound will be lifted allowing $\tan\beta$ to take much larger values at the expense of a strong correlation between the soft breaking parameter and m_H as depicted by Eq. (13).

4 Conclusions

In this paper, we have revisited the constraints from tree-unitarity and stability in the context of 2HDMs. The observed scalar at LHC has been identified with the lightest CP-even scalar of the model. The *alignment limit* has been imposed in view of the conformity of the LHC Higgs data with the SM predictions. These are the *new* informations that became available only after the Higgs discovery. If the Z_2 symmetry is exact in the potential, it is found that all the nonstandard masses are restricted below 1 TeV from unitarity with the upper limit on m_H being highly correlated to $\tan\beta$. The value of $\tan\beta$ is also confined within the range $1/8 < \tan\beta < 8$ from unitarity and stability. The constraints from flavor data severely restrict the region with $\tan\beta < 1$. Therefore, for an exact Z_2 symmetry, $\tan\beta$ is bounded within a very narrow range of $1 < \tan\beta < 8$ when a light charged scalar with mass around 400 GeV is looked for.

In the presence of an appropriate soft breaking parameter the upper bound on $\tan\beta$ will be diluted. However, for large values of $\tan\beta$, the unitarity and stability conditions will render a strong correlation between the soft breaking parameter and m_H as appears in Eq. (13). It is also worth noting that the value of $\mu_{\gamma\gamma}$ can play a crucial role in the presence of soft breaking. For example, if $\mu_{\gamma\gamma}$ is measured to be consistent with the SM expectation with 5% accuracy then one can conclude $m_{H^+}^2 \approx 1/2\lambda_5 v^2$ [13] for any value of $\tan\beta$. Thus, for large values of $\tan\beta$ one may expect $m_H^2 \approx m_{H^+}^2 \approx 1/2\lambda_5 v^2$. In this limit, the heavier nonstandard scalars truly decouple from the low energy observables. Thus, as has been emphasized in [13], proper decoupling of the nonstandard scalars necessitates the presence of a soft breaking term in the scalar potential.

To sum up, when flavor constraints are superimposed on the constraints from unitarity and stability, the value of $\tan\beta$ is restricted within a very narrow range of $1 < \tan\beta < 8$ for 2HDMs with exact Z_2 symmetry. Larger values of $\tan\beta$ can be allowed by introducing suitable soft breaking parameter in the scalar potential, but the theoretical and experimental constraints impose certain correlations between nonstandard masses and the soft breaking parameter. This makes the theory much more predictive in the large $\tan\beta$ region.

Acknowledgements: I thank G. Bhattacharyya for many helpful discussions during different stages of this work. I also thank Department of Atomic Energy, India for financial support.

References

- [1] G. Branco, P. Ferreira, L. Lavoura, M. Rebelo, M. Sher, et al., *Theory and phenomenology of two-Higgs-doublet models*, *Phys.Rept.* **516** (2012) 1–102, [[arXiv:1106.0034](https://arxiv.org/abs/1106.0034)].
- [2] S. L. Glashow and S. Weinberg, *Natural Conservation Laws for Neutral Currents*, *Phys.Rev.* **D15** (1977) 1958.
- [3] E. Paschos, *Diagonal Neutral Currents*, *Phys.Rev.* **D15** (1977) 1966.
- [4] B. W. Lee, C. Quigg, and H. Thacker, *Weak Interactions at Very High-Energies: The Role of the Higgs Boson Mass*, *Phys.Rev.* **D16** (1977) 1519.

- [5] J. Maalampi, J. Sirkka, and I. Vilja, *Tree level unitarity and triviality bounds for two Higgs models*, *Phys.Lett.* **B265** (1991) 371–376.
- [6] S. Kanemura, T. Kubota, and E. Takasugi, *Lee-Quigg-Thacker bounds for Higgs boson masses in a two doublet model*, *Phys.Lett.* **B313** (1993) 155–160, [[hep-ph/9303263](#)].
- [7] A. G. Akeroyd, A. Arhrib, and E.-M. Naimi, *Note on tree level unitarity in the general two Higgs doublet model*, *Phys.Lett.* **B490** (2000) 119–124, [[hep-ph/0006035](#)].
- [8] J. Horejsi and M. Kladiva, *Tree-unitarity bounds for THDM Higgs masses revisited*, *Eur.Phys.J.* **C46** (2006) 81–91, [[hep-ph/0510154](#)].
- [9] B. Gorcezyca and M. Krawczyk, *Tree-Level Unitarity Constraints for the SM-like 2HDM*, [arXiv:1112.5086](#).
- [10] B. Swiezewska, *Yukawa independent constraints for two-Higgs-doublet models with a 125 GeV Higgs boson*, *Phys.Rev.* **D88** (2013), no. 5 055027, [[arXiv:1209.5725](#)].
- [11] N. Chakrabarty, U. K. Dey, and B. Mukhopadhyaya, *High-scale validity of a two-Higgs doublet scenario: a study including LHC data*, [arXiv:1407.2145](#).
- [12] J. F. Gunion, H. E. Haber, G. L. Kane, and S. Dawson, *The Higgs Hunter’s Guide*, *Front.Phys.* **80** (2000) 1–448.
- [13] G. Bhattacharyya and D. Das, *Nondecoupling of charged scalars in Higgs decay to two photons and symmetries of the scalar potential*, *Phys. Rev.* **D91** (2015), no. 1 015005, [[arXiv:1408.6133](#)].
- [14] J. F. Gunion and H. E. Haber, *The CP conserving two Higgs doublet model: The Approach to the decoupling limit*, *Phys.Rev.* **D67** (2003) 075019, [[hep-ph/0207010](#)].
- [15] **ATLAS** Collaboration, *ATLAS-CONF-2014-009*, <https://atlas.web.cern.ch/Atlas/GROUPS/PHYSICS/CONFNOTES/ATLAS-CONF-2014-009/>.
- [16] **CMS** Collaboration, *CMS-PAS-HIG-14-009*, <http://cds.cern.ch/record/1728249?ln=en>.
- [17] O. Eberhardt, U. Nierste, and M. Wiebusch, *Status of the two-Higgs-doublet model of type II*, *JHEP* **1307** (2013) 118, [[arXiv:1305.1649](#)].
- [18] B. Coleppa, F. Kling, and S. Su, *Constraining Type II 2HDM in Light of LHC Higgs Searches*, *JHEP* **1401** (2014) 161, [[arXiv:1305.0002](#)].
- [19] C.-Y. Chen, S. Dawson, and M. Sher, *Heavy Higgs Searches and Constraints on Two Higgs Doublet Models*, *Phys.Rev.* **D88** (2013) 015018, [[arXiv:1305.1624](#)].
- [20] N. Craig, J. Galloway, and S. Thomas, *Searching for Signs of the Second Higgs Doublet*, [arXiv:1305.2424](#).
- [21] B. Dumont, J. F. Gunion, Y. Jiang, and S. Kraml, *Constraints on and future prospects for Two-Higgs-Doublet Models in light of the LHC Higgs signal*, *Phys.Rev.* **D90** (2014) 035021, [[arXiv:1405.3584](#)].
- [22] J. Bernon, B. Dumont, and S. Kraml, *Status of Higgs couplings after Run-1 of the LHC using Lilith 1.0*, [arXiv:1409.1588](#).
- [23] K. Klimenko, *On Necessary and Sufficient Conditions for Some Higgs Potentials to Be Bounded From Below*, *Theor.Math.Phys.* **62** (1985) 58–65.
- [24] M. Maniatis, A. von Manteuffel, O. Nachtmann, and F. Nagel, *Stability and symmetry breaking in the general two-Higgs-doublet model*, *Eur.Phys.J.* **C48** (2006) 805–823, [[hep-ph/0605184](#)].

- [25] **LEP Higgs Working Group for Higgs boson searches, ALEPH Collaboration, DELPHI Collaboration, L3 Collaboration, OPAL Collaboration**, *Search for charged Higgs bosons: Preliminary combined results using LEP data collected at energies up to 209-GeV*, [hep-ex/0107031](#).
- [26] G. Bhattacharyya, D. Das, P. B. Pal, and M. Rebelo, *Scalar sector properties of two-Higgs-doublet models with a global $U(1)$ symmetry*, *JHEP* **1310** (2013) 081, [[arXiv:1308.4297](#)].
- [27] A. Biswas and A. Lahiri, *Masses of physical scalars in two Higgs doublet models*, [arXiv:1412.6187](#).
- [28] **CMS Collaboration**, V. Khachatryan et al., *Observation of the diphoton decay of the Higgs boson and measurement of its properties*, *Eur.Phys.J.* **C74** (2014), no. 10 3076, [[arXiv:1407.0558](#)].
- [29] **ATLAS Collaboration**, G. Aad et al., *Measurement of Higgs boson production in the diphoton decay channel in pp collisions at center-of-mass energies of 7 and 8 TeV with the ATLAS detector*, [arXiv:1408.7084](#).
- [30] **Heavy Flavor Averaging Group Collaboration**, Y. Amhis et al., *Averages of B -Hadron, C -Hadron, and tau-lepton properties as of early 2012*, [arXiv:1207.1158](#).
- [31] **Particle Data Group Collaboration**, K. Olive et al., *Review of Particle Physics*, *Chin.Phys.* **C38** (2014) 090001.
- [32] M. Misiak et al., *Updated NNLO QCD predictions for the weak radiative B -meson decays*, *Phys. Rev. Lett.* **114** (2015), no. 22 221801, [[arXiv:1503.01789](#)].
- [33] A. Wahab El Kaffas, P. Osland, and O. M. Ogreid, *Constraining the Two-Higgs-Doublet-Model parameter space*, *Phys. Rev.* **D76** (2007) 095001, [[arXiv:0706.2997](#)].
- [34] F. Mahmoudi and O. Stal, *Flavor constraints on the two-Higgs-doublet model with general Yukawa couplings*, *Phys.Rev.* **D81** (2010) 035016, [[arXiv:0907.1791](#)].
- [35] O. Deschamps, S. Descotes-Genon, S. Monteil, V. Niess, S. T’Jampens, et al., *The Two Higgs Doublet of Type II facing flavour physics data*, *Phys.Rev.* **D82** (2010) 073012, [[arXiv:0907.5135](#)].